DIRECTION-OF-ARRIVAL ESTIMATION OF NONSTATIONARY SIGNALS EXPLOITING SIGNAL CHARACTERISTICS

Yimin D. Zhang†, *Moeness G. Amin*† *and Braham Himed*‡

† Center for Advanced Communications, Villanova University, Villanova, PA 19085, USA
‡ Air Force Research Laboratory, AFRL/RYMD, Dayton, OH 45433, USA

ABSTRACT

This paper proposes a novel approach for the direction-of-arrival (DOA) estimation of nonstationary signals. The proposed technique assumes signals characterized by instantaneous frequency (IF) laws and exploits IF estimates for improved DOA estimation. The focus is on achieving resolved and accurate DOA estimates for weak and closely spaced sources which demonstrate highly nonlinear and closely spaced time-varying IF signatures. The DOA estimation of a particular source is achieved by demodulation or stationarization of its signature and separating it from those of other sources. The source separation relies on the narrowband property of the demodulated signature and leads to improved signal-to-noise ratio (SNR). The effectiveness of the proposed technique, in providing robust DOA estimation, is verified by simulation results.

1. INTRODUCTION

Time-frequency (TF) analysis is a powerful technique to analyze nonstationary signals. In particular, for nonstationary signals that can be characterized by their instantaneous frequencies (IFs), selection of TF regions around the IFs retains high signal energy concentration and thus results in significant signal-to-noise ratio (SNR) enhancement [1]. When a multi-sensor array is involved, a spatial TF distribution (STFD) matrix constructed from these selected TF regions offers more robust signal and noise subspace estimation. Within this framework, subspace-based direction-of-arrival (DOA) estimation techniques achieve improved performance, especially when signal arrivals are of weak power and/or closely spaced [2, 3, 4]. In addition, the capability of selecting specific TF regions allows source discrimination, enabling improved DOA estimation with a reduced number of sensors.

The capabilities of SNR enhancement and source discrimination are limited by the size of the window emphasizing the local properties [1, 3]. Typical bilinear TF representations achieve best resolution in the joint TF domain when the IF signatures have linear behaviors and long windows can be applied. For signals whose IFs are highly nonlinear, the achievable SNR gain, associated with short windows, may be limited. Further, for close IF signatures, arising due to multiple sources, target maneuvering behaviors, or multipath propagation, applying a small window may not successfully separate the IF signatures in the TF domain for source discrimination. The problem becomes even more compounded with the existence of cross-terms due to bilinear TF transforms.

The objective of this paper is to achieve resolved and accurate DOA estimation for challenging scenarios associated with weak and closely spaced sources which have highly nonlinear and closely separated IF signatures. Note that, in practice, the source signals can be either active emitters or maneuvering targets, reflecting signals transmitted from a radar. In the latter case, the IF signatures are due to the Doppler frequency of moving/maneuvering targets and possibly depend on the environment (e.g., the ionosphere variation in over-the-horizon radar systems [5]). In this paper, we propose a novel approach, referred to as the signal filtering MUSIC (SF-MUSIC), which exploits the IF estimates for coherent array processing. Toward this end, an estimate of the IF signatures is first obtained for each source signal from the data received at all antennas [6, 7]. One IF signature is selected for respective source DOA estimation. Demodulation or stationarization of this signature is then performed by multiplying the data by the conjugate of the instantaneous phase estimate. The stationarized signature is, therefore, confined within a narrow vicinity of the direct current (DC) frequency [7]. Long window and lowpass filters (LPFs) can then be applied to separate the signature of interest from those of other sources and concurrently enhance SNR. Notice that the same waveform is applied at all array sensors for stationarization and, therefore, the spatial phase information across the array is preserved. Unlike the bilinear TF analysis based techniques, the proposed SF-MUSIC technique only involves linear operations and, as a result, do not generate cross-term TF artifacts.

As is well known, DOA estimation performance degrades rapidly when the sources have close angular separation [8, 9]. The above source discrimination, through signature demodulation and filtering, allows DOA estimation to be processed for individual sources. The proposed SF-MUSIC achieves robust DOA estimation capability of multiple nonstationary sources in a low SNR environment and extends the applicability of array signal processing to a class of DOA estimation problems which cannot be effectively tackled by existing techniques.

It is important to notice the difference between the signal IF characteristics used in the proposed SF-MUSIC technique and the known signal waveforms used in maximum

The work of Y. D. Zhang and M. G. Amin is supported in part by a subcontract with Dynetics, Inc. for research sponsored by the Air Force Research Laboratory (AFRL) under Contract FA8650-08-D-1303.

likelihood (ML) DOA estimations [10, 11]. The assumption made in this paper is much more relaxed. Unlike the ML methods with known waveforms [10, 11] that assume precise knowledge of waveforms of all signals and is sensitive to phase estimation errors, our method only assumes IF estimates with high, but not necessarily perfect, estimation accuracies. In practice, IF and phase estimation is limited by frequency resolution, noise and other perturbations. As such, our method is applicable to situations where the signal waveforms cannot be perfectly reconstructed due to IF and phase estimation inaccuracy.

Notations. A lower (upper) case bold letter denotes a vector (matrix). $\mathbb{E}[\cdot]$ represents statistical mean operation. $(\cdot)^T$ and $(\cdot)^H$ respectively denote transpose and conjugate transpose operations. $\mathbf{I}_N$ expresses the $N \times N$ identity matrix, and $\mathbf{1}$ denotes a vector with all 1 elements. In addition, $\mathbb{C}^{N\times M}$ denotes the complete set of $N \times M$ complex entries, and $[\mathbf{A}]_{m,n}$ denotes the (m, n)th element of matrix $\mathbf{A}$.

2. SIGNAL MODEL

Consider K narrowband nonstationary signals impinging on an array consisting of N sensors. For simplicity and without loss of generality, we assume a one-dimensional (1-D) DOA estimation problem, i.e., only the azimuth angle is considered. The $N \times 1$ received data vector $\mathbf{x}(t)$ and the $K \times 1$ source signal vector $\mathbf{d}(t)$ are related by

$$\mathbf{x}(t) = \mathbf{A}(\boldsymbol{\theta})\mathbf{d}(t) + \mathbf{n}(t), \quad t = 1, ..., T, \tag{1}$$

where t is the time index, $\mathbf{A}(\boldsymbol{\theta}) = [\mathbf{a}(\theta_1), ..., \mathbf{a}(\theta_K)] \in \mathbb{C}^{N\times K}$ is the mixing matrix that holds the steering vectors of the K signals, $\boldsymbol{\theta} = [\theta_1, ..., \theta_K]$, and $\mathbf{a}(\theta_k)$ is the steering vector for the kth source, $d_k(t)$, that arrives from direction θ_k. T is the number of observation samples. $\mathbf{n}(t) \in \mathbb{C}^{N\times 1}$ is an additive noise vector that consists of independent and identically distributed (i.i.d.) zero-mean, white and complex Gaussian processes with variance $\sigma_n^2\mathbf{I}_N$. The noise elements are assumed to be independent of the signals.

In this paper, we assume that each element of $\mathbf{d}(t) = [d_1(t), ..., d_K(t)]^T$ is a mono-component frequency modulated (FM) signal. Depending on the signal waveforms, the FM signal can be modeled as a sinusoidal, linear FM (LFM, also referred to as a chirp), higher-order polynomial phase signal (PPS), or any kind of mono-component signals with clear IFs. In our work, the FM signals may be subject to slowly time-varying amplitudes due to, for example, target radar cross-section (RCS) fluctuation associated with target maneuvering or channel variation in a dynamic environment (e.g., ionosphere variation in over-the-horizon radar (OTHR) systems). Thus, the FM signals can be modeled as

$$\mathbf{d}(t) = [d_1(t), ..., d_K(t)]^T = [D_1(t)e^{j\psi_1(t)}, ..., D_k(t)e^{j\psi_K(t)}]^T, \tag{2}$$

where $D_k(t)$ and $\psi_k(t)$ are the constant or slowly time-varying amplitude and time-varying phase of the kth source signal. For each sampling time t, $d_k(t)$ has an IF of $f_k(t) = d\psi_k(t)/(2\pi dt)$, provided that the frequency perturbation due to the amplitude variation is insignificant.

3. PROPOSED TECHNIQUE

The proposed technique consists of the following main steps: IF signature estimation, signal stationarization, signal filtering, and DOA estimation. The details of these steps are discussed in this section.

3.1. IF Signature Estimation

Several techniques have been developed to estimate the IF signatures of FM signals. In our problem, we deal with a mixture of multiple mono-component FM signals observed in an array of antennas. In a narrowband scenario, the mixtures observed at all the array sensors have the same IFs. Therefore, it is beneficial to combine, coherently or noncoherently, the data received across the array, especially when the signals are very noisy. Space-time adaptive processing (STAP) is usually performed as means of coherent combining [12]. On the other hand, the summation of bilinear TF distributions (or the magnitude of linear TF distributions) over all array antennas yields noncoherent signal signature enhancement [13, 14]. It is also shown in [15, 16, 17] that the data received at multiple sensors of an array or MIMO radar platforms can be used to enhance autoterm components against crossterms and noise.

For multi-component FM signals, parametric methods that estimate the IF through polynomial phase transform or Hough transform are effective [18, 19, 20]. The warped high-order ambiguity function can be used to estimate the polynomial phase coefficients [20, 21]. An FM signal with a complicated IF law can be segmented into multiple overlapped time frames so that each segment can be represented by a low-order polynomial phase signal. The polynomial phase coefficients obtained at each time frame is merged to achieve the global phase behavior [7, 21].

In this paper, we assume that the Doppler IF signatures of all signal component have been resolved through a successful application of one of the aforementioned techniques. As a result, the IFs of all signal arrivals are estimated with high, but not necessarily perfect, accuracies.

3.2. Signal Stationarization

For a specific signal $k \in [1, ..., K]$, the phase estimate $\hat{\psi}_k(t)$ can be computed through the integral of the corresponding IF estimate $\hat{f}_k(t)$. Then, the IF signature of the kth signal can be stationarized by performing the following demodulation operation:

$$\begin{aligned}\hat{\mathbf{x}}^{[k]}(t) &= \mathbf{x}(t)e^{-j\hat{\psi}_k(t)} \\ &= \hat{D}_k(t)\mathbf{a}_k + \sum_{i=1, i\neq k}^{L} D_i(t)e^{j[\psi_i(t)-\hat{\psi}_k(t)]}\mathbf{a}(\theta_i) + \hat{\mathbf{n}}^{[k]}(t),\end{aligned} \tag{3}$$

where $\hat{D}_k(t) = D_k(t)e^{j(\psi_k(t)-\hat{\psi}_k(t))}$ and $\hat{\mathbf{n}}^{[k]}(t) = \mathbf{n}(t)e^{-j\hat{\psi}_k(t)}$. Therefore, the selected kth signal, $\hat{D}_k(t)$, becomes almost stationary, whereas the other signal components will have nonzero frequencies whenever $f_i(t) \neq \hat{f}_k(t) \approx f_k(t)$ for $i \neq k$ is satisfied.

3.3. Signal Filtering

The objective of this step is to enhance the selected signal and mitigate other signals as well as interference. If the waveforms of all signals are precisely known, we can apply the ML methods assuming known waveforms [10, 11], or achieve perfect suppression of unselected signals by projecting the received signal vector to the null space of the unselected signals.

In this paper, however, we assume that the IF and phase estimates may be perturbed due to frequency resolution, noise and other factors. Our approach is rather based on frequency-domain filtering. Due to the previous stationarization step, the selected signal now lies within a narrow vicinity of the DC frequency. Assume that the IFs of all signals do not overlap. Accordingly, the demodulated IF components, other than the selected signal, are located away from the DC frequency region and can be removed using a properly designed low-pass filter (LPF).

Since the IFs of all signals are known, one can design the LPF such that the main- and side-lobes of the unselected signals do not interfere with the selected signal. Ineffective removal or suppression of other signals causes bias in the estimated DOA of the selected signal. Further, the passband selection should consider the accuracy of the IF estimates. A narrow passband yields better SNR enhancement and signal discrimination, particularly when the IFs of unselected signals are close to that of the selected signal.

Consider for example that the entire data vector of length T is divided into $P = T/Q$ nonoverlapping segments, where Q is the segment length. Low-pass filtering is achieved by summing the data in each segment, after a proper window $\mathbf{w} = [w_1, ..., w_Q]^T$, such as the Hamming window which confines the sidelobe under -40 dB, is applied. Summing the signal $\mathbf{x}^{[k]}(t)$ with a window $\mathbf{w}$ applied in the pth segment, $p = 1, ..., P$, we obtained

$$\mathbf{y}^{[k]}(p) = \frac{1}{Q} \sum_{q=(p-1)Q+1}^{pQ} w_q \mathbf{x}^{[k]}(q) = \bar{D}_k(p)\mathbf{a}_k + \bar{\mathbf{n}}^{[k]}(p), \quad (4)$$

where

$$\bar{D}_k(p) = (1/Q) \sum_{q=(p-1)Q+1}^{pQ} w_q \hat{D}_k(q), \quad \bar{\mathbf{n}}^{[k]}(p) = (1/Q) \sum_{q=(p-1)Q+1}^{pQ} w_q \hat{\mathbf{n}}^{[k]}(q).$$

Notice in the above expression that the unselected signal components are removed due to signal filtering. Also, $\bar{D}_k$ becomes $\bar{D}_k = (1/Q)\mathbf{w}^T\mathbf{1}\hat{D}_k$ when $\hat{D}_k(t) = \hat{D}_k$ is a constant.

3.4. DOA Estimation

Because $\mathbf{y}^{[k]}(\tau)$ only involves a single source, a number of methods can be used for DOA estimation. For analytical convenience and without loss of generality, our approach is developed based upon the MUSIC technique and is referred to as SF-MUSIC. Extension to other prototype DOA estimation techniques, such as root-MUSIC and ESPRIT, is straightforward.

Construct the following covariance matrix

$$\mathbf{R}_{\mathbf{y}}^{[k]} = \sum_{p=1}^{P} \mathbf{y}^{[k]}(p)[\mathbf{y}^{[k]}(p)]^H. \quad (5)$$

Denote $\hat{\mathbf{G}}$ as the matrix that spans the noise subspace of $\mathbf{R}_{\mathbf{y}}^{[k]}$, the SF-MUSIC method identifies the DOA by finding the peak of the following pseudo spatial spectrum:

$$f(\theta) = [\mathbf{a}(\theta)^H \hat{\mathbf{G}}\hat{\mathbf{G}}^H \mathbf{a}(\theta)]^{-1}. \quad (6)$$

4. PERFORMANCE ANALYSIS

Consider a uniform linear array (ULA). When classic MUSIC is applied to $\mathbf{x}(t)$ which contains K signals, the variance of the estimated spatial frequency, $\omega_k = 2\pi f_c d \sin(\theta_k)/c$, is given by [8]

$$\mathrm{var}_{\mathrm{MU}}(\hat{\omega}_k) = \frac{1}{2T} \frac{\mathbf{a}^H(\theta_k)\mathbf{U}\mathbf{a}^H(\theta_k)}{h(\omega_k)}, \quad (7)$$

for $k = 1, ..., K$, where f_c is the carrier frequency, c is the propagation velocity, d is the interelement spacing,

$$\mathbf{U} = \sigma_n^2 \left[\sum_{i=1}^{K} \frac{\lambda_i}{(\sigma_n^2 - \lambda_i)^2} \mathbf{s}_i \mathbf{s}_i^H \right], \quad (8)$$

$h(\omega_k) = \mathbf{d}^H(\omega_k)\mathbf{G}\mathbf{G}^H\mathbf{d}(\omega_k)$, and $\mathbf{d}(\omega) = d\mathbf{a}(\theta)/d\omega$ is the derivative of the steering vector relative to the spatial frequency. $\mathbf{S} = [\mathbf{s}_1, ..., \mathbf{s}_K]$ spans the signal subspace of $\mathbf{R}_{\mathbf{x}} = \mathbb{E}[\mathbf{x}(t)\mathbf{x}^H(t)]$, and $\mathbf{G}$ spans the noise subspace of $\mathbf{R}_{\mathbf{x}}$. λ_i is the corresponding eigenvalues of $\mathbf{R}_{\mathbf{x}}$ corresponding to the ith signal subspace eigenvector, $1 \le i \le K$.

When the K signals are uncorrelated, the above result can be simplified as [8]

$$\mathrm{var}_{\mathrm{MU}}(\hat{\omega}_k) = \frac{1}{2T\gamma_k} \cdot \frac{1}{h(\omega_k)} \left[1 + \frac{[\mathbf{A}^H\mathbf{A}]^{-1}_{k,k}}{\gamma_k} \right], \quad (9)$$

where γ_k is the input SNR of the kth signal. In particular, for a single-source scenario (K=1), $[\mathbf{A}^H\mathbf{A}]_{k,k} = \mathbf{a}^H(\theta_k)\mathbf{a}(\theta_k) = N$, then we have

$$\mathrm{var}_{\mathrm{MU}}(\hat{\omega}_k) = \frac{1}{2T\gamma_k} \cdot \frac{1}{h(\omega_k)} \left[1 + \frac{1}{N\gamma_k} \right]. \quad (10)$$

For the proposed SF-MUSIC technique, by noting the fact that only a single signal is chosen from multiple sources in presence, and a single data is yielded in each of the P non-overlapping segments, the variance of the estimated spatial frequency becomes

$$\mathrm{var}_{\mathrm{SF}}(\hat{\omega}_k) = \frac{1}{2P\tilde{\gamma}_k} \cdot \frac{1}{\tilde{h}(\omega_k)} \left[1 + \frac{1}{N\tilde{\gamma}_k} \right], \quad (11)$$

where $\tilde{\gamma}_k$ is the SNR of the kth source as evaluated in (4) for each sensor, and $\tilde{h}(\omega_k) = \mathbf{d}^H(\omega_k)\tilde{\mathbf{G}}\tilde{\mathbf{G}}^H\mathbf{d}(\omega_k)$ is similarly defined with respect to $\mathbf{y}^{[k]}(p)$ with a single source selected.

For constant $\hat{D}_k(t) = D_k$, the SNR $\tilde{\gamma}_k$ is evaluated as

$$\tilde{\gamma}_k = \frac{\bar{D}_k^2}{\mathbb{E}\left|\bar{n}_l^{[k]}(p)\right|^2} = \frac{\left|\sum_{q=1}^{Q} w_q\right|^2 D_k^2}{\left|\sum_{q=1}^{Q} w_q^2\right| \sigma_n^2} = \beta Q \gamma_i, \quad (12)$$

where β is a scalar depending on the window being used. For a rectangular window, β takes a value of 1, whereas for the Hamming window, the value of β is plotted in Fig.

1 for different window length. When a large size window is used, this would only yield 16% of RMSE performance degradation. Substituting (12) to (11), and noticing $T = PQ$, we have

$$\text{var}_{\text{SF}}(\hat{\omega}_k) = \frac{1}{2\beta T \gamma_k} \cdot \frac{1}{\tilde{h}(\omega_k)} \left[1 + \frac{1}{\beta N Q \gamma_k} \right]. \tag{13}$$

5. REMARKS

Note that, for LFM signals, the fractional Fourier transform (FrFT) rotates the signal signatures in the TF plane and thus enables their stationarization. In this sense, the proposed technique can be considered as an extension of FrFT-based DOA estimation techniques (e.g., [22]).

On the other hand, the proposed technique is much simpler than the TF-MUSIC [3, 23] because computations of the STFD matrices are not required. For highly nonlinear Doppler signatures, the applicable window size in the TF-MUSIC is limited by the time-varying Doppler signature and the TF kernel. SF-MUSIC can use a much larger window size due to the removal of the nonlinear phase components. Notice that the window size not only affects the achievable SNR, but also determines the frequency-domain resolution and thus the signal discrimination capability.

6. SIMULATION RESULTS

Two simulations are performed to compare the performance of the proposed SF-MUSIC to conventional MUSIC. A 6-element uniform linear array with half-wavelength interelement spacing is used for DOA estimation.

In the first experiment, we consider a single source, which shows a sinusoidal IF signature:

$$f(t) = f_m \sin(2\pi t/T), \tag{14}$$

where f_m is set to 0.4, and T is the number of samples, which is chosen to be 512 in our example. The IF signature of the source signal is shown in Fig. 2(a). The short-time Fourier transform (STFT) magnitude of the noise-free signal is shown in Fig. 2(b), where the window length is 64. Note that a large window will results in data smearing in the TF domain. The STFT magnitude of the stationarized signal is shown in Fig. 2(c), where the window length is 512. The signal is well resolved with a high SNR enhancement. The RMSE of the DOA estimates is shown in 3, where the true DOA of the signal is 44^o. We assume $P = 1$, and a rectangular window of length $Q = T$ is applied for the SF-MUSIC. The results are obtained by averaging over 200 independent trials. It is evident that the SNR enhancement in the SF-MUSIC extends the linear relationship between the logarithm RMSE and the dB level of the input SNR in a low SNR regime, and outperforms the conventional MUSIC in this regime.

In the second example, two FM signals are considered. In addition to the one considered above, we add another signal which is obtained by shift the first signal by 0.0045 at the frequency domain. This difference makes the unselected signal, after stationarization, appears in the second sidelobe at the DC frequency if Fourier transform is performed with a rectangular window. The IFs of the two source signals are depicted in Fig. 4(a). The STFT magnitude of the noise-free signal received at the first array antenna is shown in Fig. 4(b), where the window is 64. The stationarized IF signatures and the corresponding STFT magnitude are respectively shown in Figs. 4(c) and 4(d), where a Hamming window with size 512 is used in the latter plot. The true DOAs of the two signals are 44^o and 46^o, respectively.

In Fig. 5, we compare the pseudo-spectra of the conventional MUSIC and the SF-MUSIC, which are computed at input SNR of 0 dB. Again $P = 1$ is assumed, and a Hamming window and a rectangular window of length $Q = T$ are respectively applied for the two sets of SF-MUSIC spectrum plots. It is clear that the conventional MUSIC does not resolve the two signals because of their close spatial separation. On the other hand, SF-MUSIC achieves resolved DOA estimation because of its source discrimination capability. SF-MUSIC using a rectangular window shows bias of the spectrum peaks towards the DOA of the other signal. The RMSE of the DOA estimates of the first signal is shown in 6. The conventional MUSIC shows a 1^o error floor over the SNR range being computed because of the unresolved DOA estimates. The SF-MUSIC methods achieve significant improvement because they take advantages of both source discrimination and SNR enhancement. SF-MUSIC with the use of a rectangular window achieves almost the same performance as in the single-source case at the low SNR regime, but it suffers from an error floor of about 0.16^o because of the sidelobe leakage from the unselected signal. SF-MUSIC using a Hamming window does not suffer from this problem over the entire SNR range being investigated, but the performance slightly degrades because of the energy loss, represented by the factor β, as discussed in Section 4.

To show the sensitivity of ML method to the estimation error of the assumed known waveforms, Fig. 6 also includes the RMSE of the ML method, where a 5^o error yields a floor of approximately 0.63^o. On the other hand, the performance of the proposed technique is not affected by a phase estimation error.

7. CONCLUSION

In this paper, we have developed a new technique for the direction-of-arrival (DOA) estimation of nonstationary signals that are characterized by their instantaneous frequencies (IFs). The proposed technique comprises four steps of IF estimation, stationarization, filtering, and DOA estimation. By exploiting coarse estimates of the IF signatures, the proposed signal-filtering based DOA estimation technique resolves closely spaced sources of closely separated IF signatures. Two simulation examples were given to demonstrate the effectiveness of the proposed technique.

REFERENCES

[1] X-G. Xia and V. Chen, "A quantitative SNR analysis for the pseudo Wigner-Ville distribution," *IEEE Trans. Signal Proc.*, vol. 47, no. 10, pp. 2891-2894, Oct. 1999.

[2] Y. Zhang, W. Mu, and M. G. Amin, "Time-frequency maximum likelihood methods for direction finding," *J. Franklin Inst.*, vol. 337, no. 4, pp. 483–497, July 2000.

[3] Y. Zhang, W. Mu, and M. G. Amin, "Subspace analysis of spatial time-frequency distribution matrices," *IEEE Trans. Signal Proc.*, vol. 49, no. 4, pp. 747–759, April 2001.

[4] M. G. Amin and Y. Zhang, "Spatial time-frequency distributions and DOA estimation," in E. Tuncer and B. Friedlander (eds), *Classical and Modern Direction of Arrival Estimation*, Academic Press, 2009.

[5] Y. D. Zhang, M. G. Amin, and B. Himed, "Altitude estimation of maneuvering targets in MIMO over-the-horizon radar," in *Proc. IEEE Sensor Array and Multichannel Signal Processing Workshop*, Stevens, NJ, June 2012.

[6] C. Ioana, M. G. Amin, Y. D. Zhang, and F. Ahmad, "Characterization of Doppler effects in the context of over-the-horizon radar," *IEEE Int. Radar Conf.*, Washington D.C., May 2010.

[7] C. Ioana, Y. D. Zhang, M. G. Amin, F. Ahmad, and B. Himed, "Time-frequency analysis of multipath Doppler signatures of maneuvering targets," in *Proc. IEEE Int. Conf. Acoust., Speech, Signal Proc.*, Kyoto, Japan, March 2012.

[8] P. Stoica and A. Nehorai, "MUSIC, maximum likelihood and Cramer-Rao bound," *IEEE Trans. Acoust., Speech, Sig. Proc.*, vol. ASSP-37, no. 5, pp. 720–741, May 1989.

[9] J. Jachner and H. Lee, "Foundamental limitations on direction finding performance for closely spaced sources," in S. Haykin (ed), *Advanced in Spectrum Analysis and Array Processing*, Pentice-Hall, 1995.

[10] J. Li and R. T. Compton, "Maximum likelihood angle estimation for signals with known waveforms," *IEEE Trans. Signal Proc.*, vol. 41, no. 9, pp.2850-2862, Sept. 1993.

[11] J. Li, B. Halder, P. Stoica, and M. Viberg, "Computationally efficient angle estimation for signals with known waveforms," *IEEE Trans. Signal Proc.*, vol. 43, no. 9, pp. 2154–2163, Sept. 1995.

[12] R. Klemm, *Principles of Space-Time Adaptive Processing*, IEE, 2002.

[13] W. Mu, M. G. Amin, and Y. Zhang, "Bilinear signal synthesis in array processing," *IEEE Trans. Signal Proc.*, vol. 51, no. 1, pp. 90–100, Jan. 2003.

[14] X. Li, Y. D. Zhang, and M. G. Amin, "Real-time tracking of bullet trajectory based on chirp transform in a multi-sensor multi-frequency radar," in *Proc. IEEE Int. Radar Conf.*, Washington D.C., May 2010.

[15] L-T. Nguyen, A. Belouchrani, K. Abed-Meraim, and B. Boashash, "Separating more sources than sensors using time-frequency distributions," *EURASIP J. Applied Signal Proc.*, vol. 2005, no. 17, pp. 2828–2847, 2005.

[16] Y. Zhang and M. G. Amin, "Blind separation of nonstationary sources based on spatial time-frequency distributions," *EURASIP J. Applied Signal Proc.*, vol. 2006, article ID 64785, 13 pages, 2006.

[17] Y. D. Zhang and M. G. Amin, "MIMO radar for direction finding with exploitation of time-frequency representations," in *Proc. IEEE Int. Conf. Acoustics, Speech, and Signal Proc.*, Prague, Czech Republic, May 2011.

[18] S. Peleg and B. Porat, "Estimation and classification of polynomial-phase signals," *IEEE Trans. Inform. Theory*, vol. 37, March 1991.

[19] S. Barbarossa, "Analysis of multicomponent LFM signals by a combined Wigner-Hough transform," *IEEE Trans. Signal Proc.*, vol. 43, no. 6, pp. 1511-1515, June 1995.

[20] S. Barbarossa, A. Scaglione, and G. B. Giannakis, "Product high-order ambiguity function for multicomponent polynomial-phase signal modeling," *IEEE Trans. Signal Proc.*, vol. 46, no. 3, pp. 691-708, 1998.

[21] C. Ioana and A. Quinquis, "Time-frequency analysis using warped-based high-order phase modeling," *EURASIP J. Applied Signal Proc.*, vol. 2005, no. 17, pp. 2856–2873, Sept. 2005.

[22] H. Qu, R. Wang, W. Qu, and P. Zhao, "Research on DOA estimation of multi-component LFM signals based on the FRFT," *Wireless Sensor Network*, vol. 2009, no. 3, pp. 171–181, 2009.

[23] A. Belouchrani and M. G. Amin, "Time-frequency MUSIC," *IEEE Signal Proc. Lett.*, vol. 6, no. 5, pp. 109–110, May 1999.

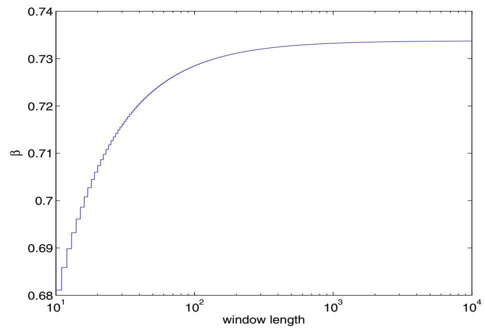

Figure 1: The value of β versus the window length.

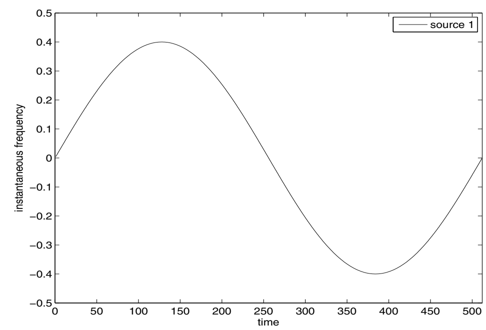

(a) IF signature

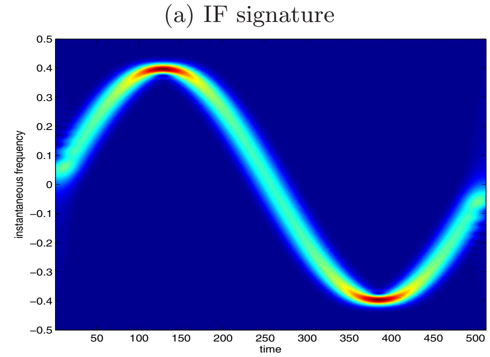

(b) STFT magnitude of original signal (window length 64)

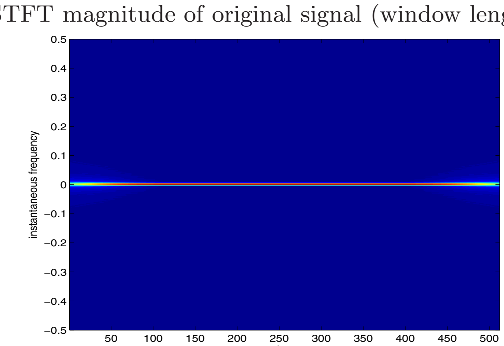

(c) STFT magnitude of stationarized signal (window length 512)

Figure 2: IF signature of the source.

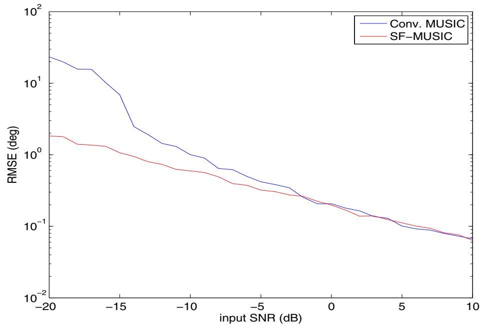

Figure 3: Comparison of RMSE of the estimated DOA (single-source case).

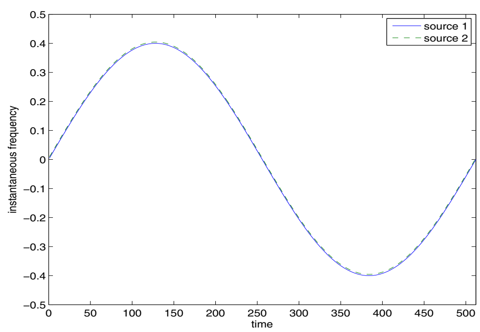

(a) IF signatures

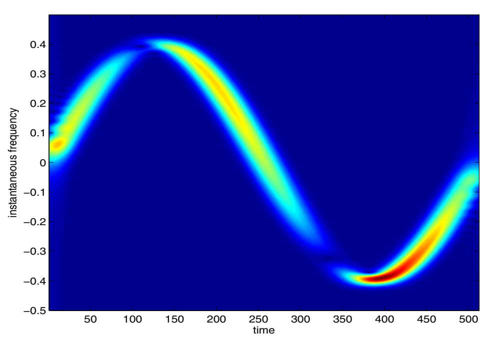

(b) STFT magnitude of original signals (window length 64)

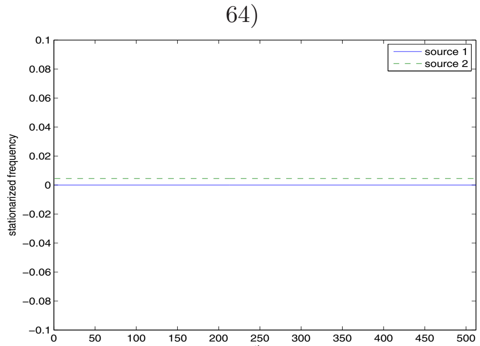

(c) IF signatures stationarized by the 1st signal

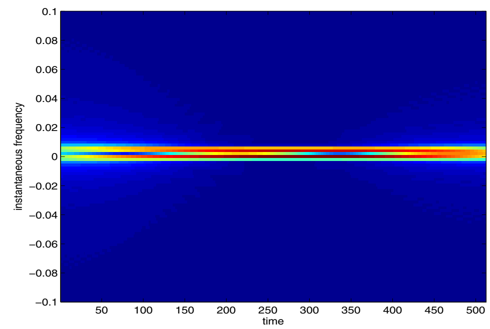

(d) STFT magnitude of stationarized signals (window length 512)

Figure 4: IF signatures of the two sources.

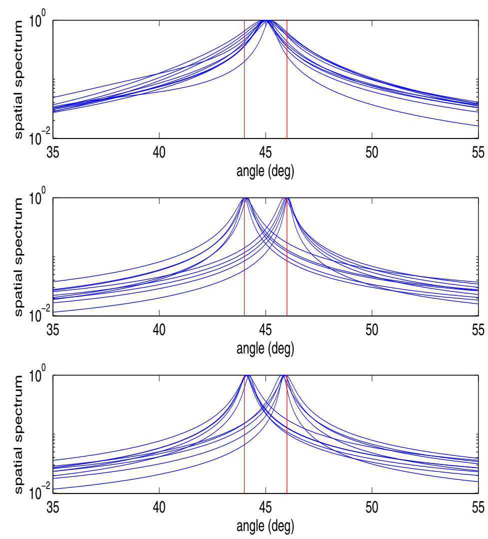

Figure 5: Pseudo-spectra of conventional MUSIC and SF-MUSIC (SNR=0dB). Top: conventional MUSIC; Middle: SF-MUSIC with Hamming window; Bottom: SF-MUSIC with rectangular window.

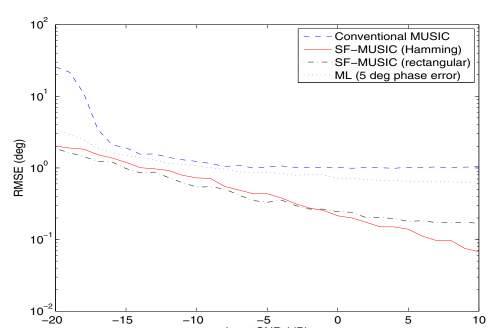

Figure 6: Comparison of RMSE of the estimated DOA (two source case).